Cellular/Molecular

Coassembly and Coupling of SK2 Channels and $mGlu_5$ Receptors

Gloria García-Negredo,[1]* David Soto,[2]* Javier Llorente,[1] Xavier Morató,[1] Koen M.O. Galenkamp,[1] Maricel Gómez-Soler,[1] Víctor Fernández-Dueñas,[1] Masahiko Watanabe,[3] John P. Adelman,[4] Ryuichi Shigemoto,[5] Yugo Fukazawa,[5] Rafael Luján,[6] and Francisco Ciruela[1]

[1]Unitat de Farmacologia, Departament Patologia i Terapèutica Experimental, Facultat de Medicina, [2]Laboratori de Neurobiologia, Institut d'Investigacions Biomèdiques de Bellvitge, Universitat de Barcelona, 08907 L'Hospitalet de Llobregat, Spain, [3]Department of Anatomy, Hokkaido University School of Medicine, Sapporo 060-0818, Japan, [4]Vollum Institute, Oregon Health & Science University, Portland, Oregon 97239, [5]Division of Cerebral Structure, National Institute for Physiological Sciences, Okazaki 444-8787, Japan, and [6]Instituto de Investigación en Discapacidades Neurológicas, Departamento de Ciencias Médicas, Facultad de Medicina, Universidad Castilla-La Mancha, 02008 Albacete, Spain

Group I metabotropic glutamate (mGlu) receptors regulate hippocampal CA1 pyramidal neuron excitability via Ca^{2+} wave-dependent activation of small-conductance Ca^{2+}-activated K^+ (SK) channels. Here, we show that $mGlu_5$ receptors and SK2 channels coassemble in heterologous coexpression systems and in rat brain. Further, in cotransfected cells or rat primary hippocampal neurons, $mGlu_5$ receptor stimulation activated apamin-sensitive SK2-mediated K^+ currents. In addition, coexpression of $mGlu_5$ receptors and SK2 channels promoted plasma membrane targeting of both proteins and correlated with increased $mGlu_5$ receptor function that was unexpectedly blocked by apamin. These results demonstrate a reciprocal functional interaction between $mGlu_5$ receptors and SK2 channels that reflects their molecular coassembly.

Key words: **electron microscopy; $mGlu_5$ receptor; oligomerization; SK2 channel; apamin**

Introduction

Glutamate receptors are found throughout the mammalian CNS, where they underlie the majority of excitatory neurotransmission (Mayer and Westbrook, 1987). There are three related subclasses of ionotropic glutamate receptors (Hollmann and Heinemann, 1994) and a distinct family of G-protein-coupled metabotropic glutamate (mGlu) receptors (Pin and Duvoisin, 1995). Among the mGlu receptors, eight subtypes have been identified and categorized into three groups on the basis of their sequence homology, pharmacological profiles, and signal transduction pathways (Pin and Duvoisin, 1995). Group I includes $mGlu_1$ and $mGlu_5$ receptors, which respond to quisqualic acid as their most potent agonist and are coupled to G_q/G_{11} proteins, thus leading to phospholipase C stimulation, IP_3 formation, and mobilization of Ca^{2+} from intracellular stores (Pin and Duvoisin, 1995). In the brain, $mGlu_5$ receptors are highly expressed in the hippocampus, where they are mainly found at postsynaptic sites, showing perisynaptic localization within dendritic spines of pyramidal cells (Lujan et al., 1996). The postsynaptic activation of $mGlu_5$ receptors may modulate ion channel activity to increase the excitability of central neurons (Mannaioni et al., 2001).

Calcium-activated K^+ (K_{Ca}) channels may be divided into two subfamilies based on sequence homology and gating mechanism (Stocker, 2004). The small-conductance Ca^{2+}-activated K^+/intermediate conductance (SK/IK) channels ($K_{Ca}2/3$) are strictly Ca^{2+} dependent and calcium gating is engendered by coassembly of the pore-forming subunits with calmodulin (Xia et al., 1998; Stocker, 2004). The three different SK channel subtypes are widely expressed throughout the brain while IK channel expression is very limited (Stocker, 2004). In hippocampus, apamin-sensitive SK2-containing channels are expressed throughout the dendrites of CA1 pyramidal neurons. In spines apamin-sensitive SK2-containing channels are localized to the postsynaptic membrane as well as perisynaptic sites (Ballesteros-Merino et al., 2012). The synaptic SK2-containing channels modulate synaptic responses (Faber et al., 2005; Ngo-Anh et al., 2005) and their protein kinase A (PKA)-dependent endocytosis contributes to the expression of long-term potentiation (Lin et al., 2008). Interestingly, in layer V pyramidal neurons, $mGlu_5$ receptor activity

Received May 14, 2014; revised Sept. 2, 2014; accepted Sept. 8, 2014.

Author contributions: D.S., V.F.-D., J.P.A., R.L., and F.C. designed research; G.G.-N., D.S., J.L., X.M., K.M.O.G., M.G.-S., R.L., and F.C. performed research; M.W., J.P.A., R.S., and Y.F. contributed unpublished reagents/analytic tools; R.L. and F.C. analyzed data; V.F.-D., J.P.A., R.L., and F.C. wrote the paper.

This work was supported by Grants SAF2011-24779 and PCIN-2013-019-C03-03 from the Ministerio de Economía y Competitividad and Institució Catalana de Recerca i Estudis Avançats Academia 2010 from the Catalan Institution for Research and Advanced Studies to F.C.; by a grant from the Spanish Ministry of Education and Science (BFU-2012-38348) to R.L., and a Consolider-Ingenio CSD2008-00005 grant from the Ministerio de Ciencia e Innovación to F.C. and R.L. D.S. was supported by the Ramón y Cajal program (RyC-2010-05979). V.F.-D., M.G.-S., and F.C. belong to the Neuropharmacology and Pain accredited research group (Generalitat de Catalunya, 2009 SGR 232). We thank Esther Castaño and Benjamín Torrejón, from the Scientific and Technical Services-Bellvitge Campus of the University of Barcelona for the technical assistance, and to Paola Pedarzani from the University College of London for the help with the design of the electrophysiological experiments.

*G.G.-N. and D.S. contributed equally to this work.

The authors declare no competing financial interests.

Correspondence should be addressed to any of the following: Rafael Luján at the above address. E-mail: Rafael.Lujan@uclm.es; or John P. Adelman at the above address. E-mail: adelman@ohsu.edu; or Francisco Ciruela at the above address. E-mail: fciruela@ub.edu.

DOI:10.1523/JNEUROSCI.2038-14.2014

 0270-6474/14/3314793-10$15.00/0

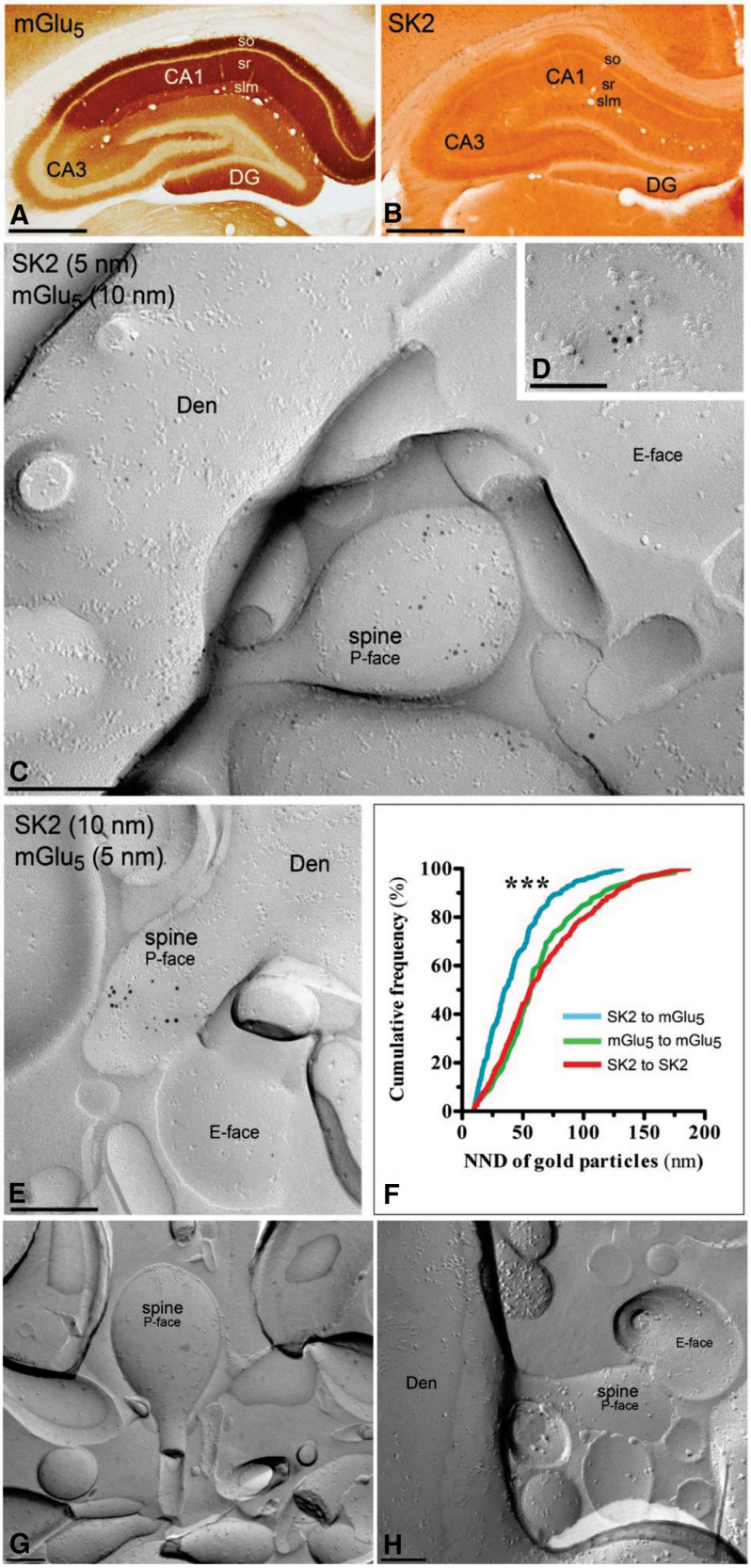

Figure 1. Codistribution of SK2 channels and mGlu$_5$ receptors in the hippocampus. ***A***, ***B***, Light micrographs showing immunoreactivity for mGlu$_5$ receptors (***A***) and SK2 channels (***B***) in the hippocampus. At the regional level, mGlu$_5$ receptors and SK2 channels show similar patterns of expression and distribution. Immunoreactivity for both mGlu$_5$ receptors and SK2 channels is intense in the neuropile of strata oriens (so) and radiatum (sr), being weaker in the stratum lacunosum-moleculare (slm) and unlabeled in the pyramidal cell layer. ***C–E***, Coclustering of SK2 channels and mGlu$_5$ receptors in dendritic spines of CA1 pyramidal cells using the SDS-FRL technique. Freeze-fracture replicas prepared from mouse hippocampus were labeled with 5 nm (small black dots) and 10 nm (bold black dots), or with 10 and 5 nm (***E***), immunoparticles to detect SK2 channels and mGlu$_5$ receptors. Both SK2 channels and mGlu$_5$ receptors are immunolabeled with antibodies directed against epitopes at the intracellular C terminus, so the two proteins can be detected at the protoplasmic face (P-face) of the plasma membrane. The exoplasmic face (E-face) is free of any immunolabeling. Clusters of immunoparticles for SK2 channels were detected in dendritic spines in the stratum radiatum in close proximity or intermingled with mGlu$_5$ receptors. ***F***, Quantitative analysis using the SDS-FRL technique, showing the nearest neighbor distance (NND) among the same and different type of labeling. The distance between immunoparticles for SK2 channels and mGlu$_5$ receptors are statistically (***$p < 0.001$, 1-way ANOVA with a Bonferroni's *post hoc* test) shorter than distances between immunoparticles for SK2 channels or for mGlu$_5$ receptors. Thus, this analysis demonstrated a spatial association between SK2 channels and mGlu$_5$ receptors. ***G***, ***H***, The antibody specificity was controlled and confirmed in replicas of SK2 channel-null mice (***G***) or mGlu$_5$ receptor-null mice (***H***) that were free of any immunolabeling. Den, Dendritic shafts of pyramidal cells. Scale bars: ***A***, ***B***, 0.5 cm; ***C***, ***E***, ***G***, 0.2 μm; ***D***, ***H***, 0.1 μm.

induces a long-term potentiation of intrinsic excitability that is mediated by decreased SK channel activity (Sourdet et al., 2003).

Here we examined the relationship between mGlu$_5$ receptors and SK2 channels. The results show that the two proteins are very closely localized in spines of hippocampal pyramidal neurons, and they coassemble into stable complexes in the hippocampus and in transfected cells. Moreover, mGlu$_5$ receptor stimulation activates SK2 channels and, surprisingly, imparts apamin sensitivity to mGlu$_5$ receptors.

Materials and Methods

Plasmids constructs. The rat SK2 (SK2 short isoform; GenBank/European Molecular Biology Laboratory/DNA Database of Japan accession no. U69882; Köhler et al., 1996) was fused with the cyan fluorescent protein (CFP) at the N terminus (i.e., SK2^{CFP}) and then the yellow fluorescent protein (YFP) was incorporated at the C terminus (i.e., SK2$^{YFP/CFP}$). The mGlu$_5$ receptor constructs containing C-terminal YFP or the *Renilla* luciferase (*R*luc; mGlu$_5^{YFP}$ and mGlu$_5^{Rluc}$, respectively) were described previously (Gandia et al., 2008; Cabello et al., 2009).

Immunohistochemistry for electron microscopy. SDS-digested freeze-fracture replica labeling (SDS-FRL) was performed with some modifications (Fujimoto, 1995). Adult C57BL/6 mice of either sex were anesthetized with sodium pentobarbital and subjected to transcardiac perfusion with formaldehyde (0.5%) in 0.1 M sodium phosphate buffer. The hippocampi were dissected and cut into sections

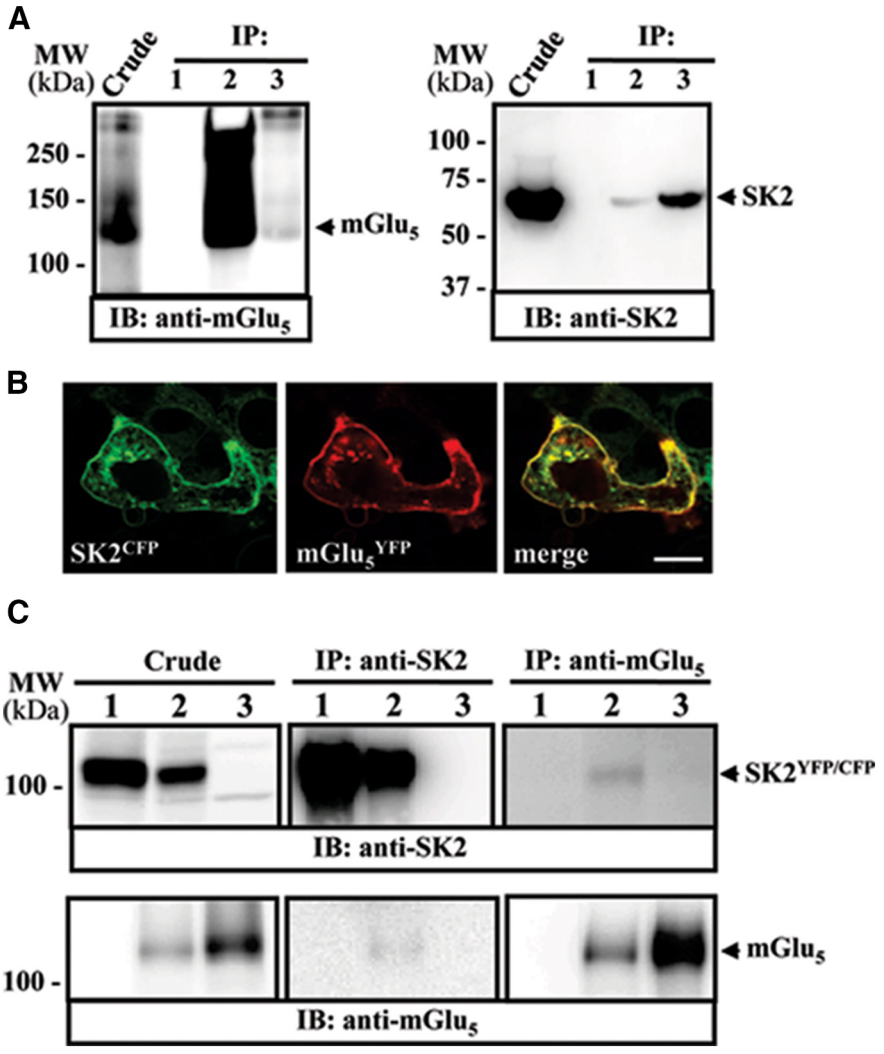

Figure 2. Association of mGlu$_5$ receptors and SK2 channels. ***A***, Coimmunoprecipitation of mGlu$_5$ receptors and SK2 channels from rat hippocampus. Solubilized extracts from rat hippocampus were subjected to immunoprecipitation analysis using rabbit anti-flag antibody (2 μg; lane 1), rabbit anti-mGlu$_5$ receptor antibody (2 μg; lane 2), and rabbit anti-SK2 channel antibody (2 μg; lane 3). Extracts (Crude) and immunoprecipitates (IP) were analyzed by SDS-PAGE and immunoblotted (IB) using a rabbit anti-mGlu$_5$ receptor antibody (1 μg/ml) or guinea pig anti-SK2 channel antibody (1 μg/ml). An HRP-conjugated anti-rabbit IgG TrueBlot (1:1000; IB: anti-mGlu$_5$) or an HRP-conjugated goat anti-guinea pig IgG (1:30,000; IB: anti-SK2) was used as a secondary antibody. The immunoreactive bands were visualized by chemiluminescence. ***B***, Codistribution of mGlu$_5$ receptors and SK2 channels expressed in HEK-293T cells. Cells were transiently transfected with the cDNAs encoding SK2^{CFP} channels plus the mGlu$_5^{YFP}$ receptors and analyzed by double fluorescence with a confocal microscope. Superimposition of images (merge) reveals a high codistribution of SK2^{CFP} channels and the mGlu$_5^{YFP}$ receptors. Scale bar, 10 μm. ***C***, Coimmunoprecipitation of mGlu$_5$ receptors and SK2 channels from HEK-293T cells. Cells were transiently transfected with SK2$^{YFP/CFP}$ channels (lane1), SK2$^{YFP/CFP}$ channels plus mGlu$_5$ receptors (lane2), or mGlu$_5$ receptors (lane 3) and processed for immunoprecipitation using mouse anti-GFP antibody (1 μg; IP: anti-SK2) or rabbit anti-mGlu$_5$ receptor antibody (1 μg; IP: anti-mGlu$_5$). Extracts (Crude) and immunoprecipitates (IP) were analyzed by SDS-PAGE and immunoblotted (IB) using a rabbit anti-SK2 channel antibody (1 μg/ml; IB: anti-SK2) or a rabbit anti-mGlu$_5$ receptor antibody (1 μg/ml; IB: anti-mGlu$_5$). An HRP-conjugated anti-rabbit IgG TrueBlot (1:1000) was used as a secondary antibody. The immunoreactive bands were visualized by chemiluminescence.

120 μm thick by a Microslicer (Dosaka). Replicas were obtained as described previously (Tarusawa et al., 2009). Replicas were transferred to 2.5% SDS containing 0.0625 M Tris and 10% glycerol, pH 6.8, for 16 h at 80°C with shaking, and then washed and reacted with a mixture of polyclonal guinea pig antibody for SK2 (Ballesteros-Merino et al., 2012) and polyclonal rabbit antibody for mGlu$_5$ receptors (Uchigashima et al., 2007) at 15°C overnight. Following three washes in 0.1% BSA in TBS and blocking in 5% BSA/TBS, replicas were incubated in a mixture of secondary antibodies coupled to gold particles (British Biocell International) overnight at 4°C. When one of the primary antibodies was omitted, no immunoreactivity for the omitted primary antibody was observed. After immunogold labeling, the replicas were immediately rinsed three times with 0.1% BSA/TBS, washed twice with distilled water, and picked up onto grids coated with pioloform (Agar Scientific). Ultrastructural analyses were performed in a Jeol-1010 electron microscope. To determine the distance between SK2 channel and mGlu$_5$ receptor immunoparticles, the nearest neighbor distances between the 5 nm gold particles (SK2 channels) and the 10 nm gold particles (mGlu$_5$ receptors) were measured. Distances between the two particles were then compared with distances between immunoparticles for SK2 channels alone or for mGlu$_5$ receptors.

Cell culture, transfection, and membrane preparation. HEK-293T cells were transiently transfected using either TransFectin Lipid Reagent (Bio-Rad Laboratories) or GeneJuice (EMD Chemicals). Membrane suspensions from transfected HEK-293T cells or rat hippocampus were obtained as described previously (Giménez-Llort et al., 2007). Primary hippocampal neurons were cultured from 0–3-d-old rats as previously described (Nassirpour et al., 2010). Neurons were kept at 5% CO_2, 37°C, and 95% humidity for 21 d before the experiments. AraC (5 μM; Sigma-Aldrich) was added on 3 DIV.

Coimmunoprecipitation and immunocytochemistry. For coimmunoprecipitation experiments, membranes from hippocampus obtained from rats of either sex or from transiently transfected HEK-293T cells were solubilized in ice-cold radioimmunoassay (RIPA) buffer (150 mM NaCl, 1% NP-40, 50 mm Tris, 0.5% sodium deoxycholate, and 0.1% SDS, pH 8.0) for 30 min on ice and processed as previously described (Martín et al., 2010). Immune complexes were dissociated, transferred to polyvinylidene difluoride membranes and probed with the indicated primary antibodies followed by horseradish-peroxidase (HRP)-conjugated secondary antibodies (TrueBlot; 1:1000; eBioscience). The immunoreactive bands were detected using Pierce ECL Western Blotting Substrate (Thermo Fisher Scientific) and visualized in a LAS-3000 (FujiFilm Life Science).

For immunocytochemistry, primary cultures of rat hippocampal neurons growing on coverslips were fixed in 4% paraformaldehyde for 15 min and exposed to guinea pig anti-SK2 channel antibody (1 μg/ml) plus a rabbit anti-mGlu$_5$ receptor antibody (1 μg/ml; Millipore). Primary antibodies were detected using a Cy2-conjugated donkey anti-rabbit antibody (1:200; Jackson ImmunoResearch Laboratories) and Cy3-conjugated donkey anti-guinea pig antibody (1:200; Jackson ImmunoResearch Laboratories). Coverslips were rinsed for 30 min, mounted with Vectashield immunofluorescence medium (Vector Laboratories), and examined using a Leica TCS 4D confocal scanning laser microscope (Leica Lasertechnik; Luján and Ciruela, 2001). For detection of fluorescent constructs, HEK-293T cells were fixed with 1% paraformaldehyde for 10 min. Cells on coverslips were mounted and examined as described above.

Bioluminescence resonance energy transfer and microscopic fluorescence resonance energy transfer measurements. For bioluminescence resonance energy transfer (BRET) experiments, HEK-293T cells expressing the indi-

cated constructs were rapidly washed, detached, and resuspended in HBSS buffer (137 mM NaCl, 5 mM KCl, 0.34 mM Na_2HPO_4, 0.44 mM KH_2PO_4, 1.26 mM $CaCl_2$, 0.4 mM $MgSO_4$, 0.5 mM $MgCl_2$, 10 mM HEPES, pH 7.4) containing 10 mM glucose. Cell suspensions (20 μg of protein) were distributed in duplicate into 96-well microplate black plates with transparent bottoms (Corning 3651, Corning) for fluorescence measurement, or white plates with white bottoms (Corning 3600, Corning) for BRET determination. For BRET measurement, *h*-coelenterazine substrate (Prolume) was added to a final concentration of 5 μM, and readings were performed 1 min later (POLARstar Optima plate-reader, BMG Labtech), which allowed the simultaneous integration of the signals detected with two filter settings [485 nm (440–500 nm) and 530 nm (510–560 nm)]. The BRET ratio was defined as previously described (Canals et al., 2003; Ciruela et al., 2004).

Fluorescence resonance energy transfer (FRET) between SK2^{CFP} channels and mGlu$_5^{YFP}$ receptors was determined by donor recovery after acceptor photobleaching, in which FRET is revealed as a significant increase in the fluorescence of the donor (i.e., CFP) after acceptor (i.e., YFP) photodestruction, as previously described (López-Hernández et al., 2011). In brief, transiently transfected HEK-293T cells seeded into 18-mm-diameter glass coverslips were mounted in an Attofluor holder and placed on an inverted Axio Observer microscope (Zeiss Microimaging) equipped with a 63× oil-immersion objective and a dual-emission photometry system (TILL Photonics). The cells were then illuminated with light from a polychrome V monochromator (Till Photonics). The excitation light was set at 436 ± 10 nm [beam splitter dichroic long-pass (DCLP) of 460 nm], and the excitation time was 10 ms at 10 Hz to minimize photobleaching. The emission light intensities were recorded at 535 ± 15 nm ($F_{(535)}$) and 480 ± 20 nm ($F_{(480)}$; beam splitter DCLP of 505 nm). The FRET efficiency between the donor (CFP) and acceptor (YFP) fluorophores was determined according to the following equation: $FRET_{efficiency} = 1 - (CFP_{pre}/CFP_{post})$, where CFP_{pre} and CFP_{post} are the CFP emissions ($F_{(480)}$) before and after photobleaching YFP by 15 min of illumination at 500 nm. GraphPad Prism (GraphPad Software) software was used for the data analysis.

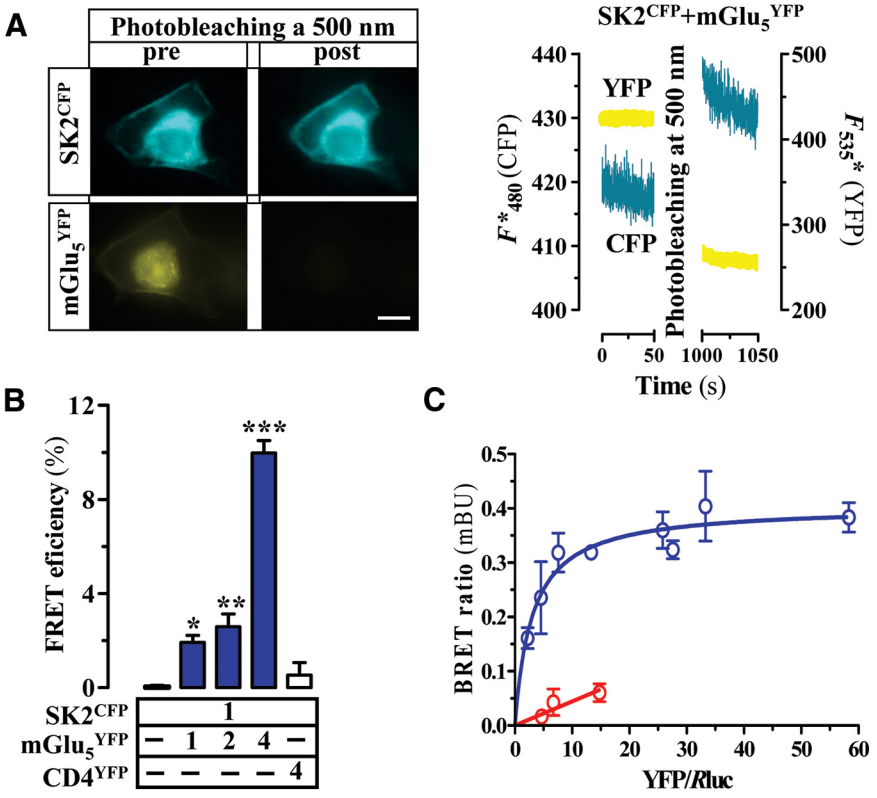

Figure 3. Oligomerization of mGlu$_5$ receptors and SK2 channels in HEK-293T cells. ***A***, Determination of the mGlu$_5$ receptor and SK2 channel oligomerization by FRET experiments in living cells. SK2^{CFP} channels and mGlu$_5^{YFP}$ receptors were expressed in HEK-293T cells, and fluorescence images of CFP and YFP were recorded before (pre) and after (post) the YFP was photobleached by 15 min of exposure to light at 500 nm to corroborate the extent of acceptor photodestruction (left). Emission intensities of SK2^{CFP} channels (480 nm, blue) and mGlu$_5^{YFP}$ receptors (535 nm, yellow) from single cells expressing both SK2^{CFP} channels and mGlu$_5^{YFP}$ receptors were recorded before and after YFP photobleaching (right) to determine the FRET efficiency. Scale bar, 10 μm. ***B***, Quantification of the FRET efficiency of different FRET pairs and expression ratios: SK2^{CFP} (1 μg) alone ($n = 10$) or in the presence of mGlu$_5^{YFP}$ (1 μg, $n = 15$; 2 μg, $n = 10$; and 4 μg, $n = 7$) or in the presence of CD4^{YFP} (4 μg; $n = 10$). The data indicate the mean ± SEM. The asterisks denote data significantly different from the SK2^{CFP} plus CD4^{YFP} cotransfection (*$p < 0.05$, **$p < 0.01$, ***$p < 0.001$, 1-way ANOVA with a Bonferroni's *post hoc* test). ***C***, BRET-based study of receptor–channel heteromerization in HEK-293T cells. BRET was measured in HEK-293T cells coexpressing mGlu$_5^{Rluc}$ receptors plus SK2$^{YFP/CFP}$ channels (blue circle) or mGlu$_5^{Rluc}$ receptors plus GABA$_2$R^{YFP} (red circle). Cotransfections were performed with increasing amounts of the YFP-tagged vectors while the mGlu$_5^{Rluc}$ was maintained constant. Both fluorescence and luminescence of each sample were measured before every experiment to confirm equal expression of *R*luc construct while monitoring the increase of YFP expression. Plotted on the *x*-axis is the fluorescence value obtained from the YFP, normalized with the luminescence value of mGlu$_5^{Rluc}$ 10 min after *h*-coelenterazine incubation. Plotted on the *y*-axis is the corresponding BRET ratio (×1000). mBU, mBRET units. Data shown are the mean ± SEM of a representative experiment performed in triplicate.

Biotinylation of cell-surface proteins. Cell-surface proteins were biotinylated as previously described (Ciruela et al., 2000). Biotinylated cell membranes were solubilized in ice-cold RIPA buffer and centrifuged at 14,000 × *g* for 20 min. The supernatant was incubated with 80 μl of streptavidin-agarose beads (Sigma-Aldrich) for 1 h with constant rotation at 4°C. The beads were washed and processed for immunoblotting.

Intracellular calcium determinations. The mGlu$_5$ receptor-mediated intracellular Ca^{2+} accumulation was assessed by means of a luciferase reporter assay as previously described (Borroto-Escuela et al., 2011) or by Fluo4. For the nuclear factor of activated T-cells (NFAT) luciferase reporter assay, Bright-Glo (Promega) was added to the transfected cells 1:1 (v/v), and the luciferase activity was determined in a POLARStar Optima plate-reader using a 30-nm-bandwidth excitation filter at 535 nm. Firefly luciferase luminescence was measured over a 15 s reaction period. *R*luc luminescence was measured as described above. Firefly luciferase values were normalized against *R*luc. For the Fluo4 determinations, transiently transfected HEK-293T cells were lifted and plated in 96-well black plates with transparent bottoms. Cells were incubated with the Fluo4-NW Calcium Assay Kit (Invitrogen) following the instructions of the manufacturer, washed with HBSS, and incubated in presence or absence of apamin (100 nM). Fluorescence signals were measured at 530 nm during 45 s while injecting L-glutamate (1 mM) and ionomycin (5 μM) at seconds 5 and 25 respectively, using a POLARstar Omega plate reader. The specific L-glutamate-induced Fluo4 signal (F) was expressed as percentage of the signal elicited by ionomycin (F_i) in each experimental condition.

IP$_1$ assay in hippocampal neurons. Hippocampal neurons growing in six-well plates were incubated with 50 mM LiCl for 10 min before being activated with the indicated compounds for 1 h. Neurons were lysed in buffer containing Phosphatase Inhibitor Cocktail 2 (Sigma-Aldrich) and the lysates transferred into a 384-well plate. Subsequently, the IP$_1$ assay components (Cisbio) were added following the manufacturer's instructions. The FRET signal, calculated as previously described (Martín et al., 2010), was transformed into the accumulated IP$_1$ using a calibration curve prepared on the same plate and presented as the fold increase over the basal levels of IP$_1$.

Electrophysiology. Coverslips with transfected cells expressing SK2^{CFP} channels plus eYFP or mGlu$_5^{YFP}$ receptors were mounted in an Attofluor

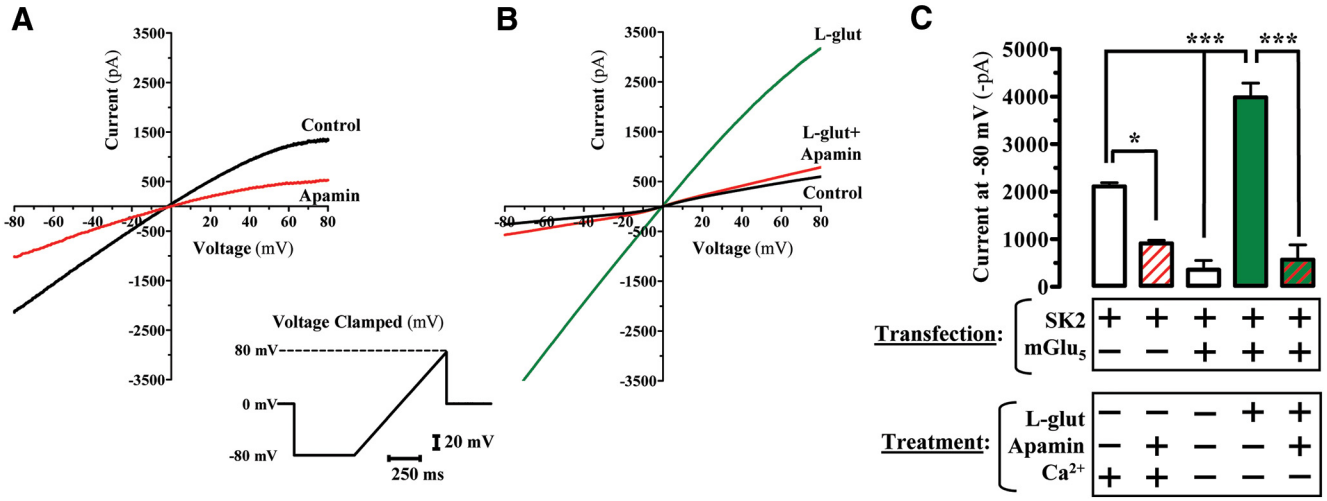

Figure 4. SK2 channel activity in HEK-293T cells. ***A***, ***B***, Representative inward rectifying current–voltage curve recorded from patch-clamp voltage-clamped HEK-293T cell transiently expressing the SK2 channels alone (***A***) or SK2 channels plus the mGlu$_5$ receptors (***B***). Cells were transiently transfected with the cDNA encoding the untagged channels and receptors plus the GFP protein to aid in the localization of transfected cells. Cells were clamped at 0 mV in a symmetrical K^+ buffer ($[K^+]i = [K^+]o$) and voltage ramps over a membrane potential range of −80 to 80 mV were performed (lower inset) in the presence (***A***) or absence (***B***) of calcium. In ***A***, electrodes were filled with an internal solution composed of the following: 120 mM KCl, 10 mM HEPES, 10 mM EGTA, 1.5 mM Na_2ATP, 9.65 mM $CaCl_2$, 2.34 mM $MgCl_2$, pH 7.4, adjusted with KOH. Cells were bathed in an external solution containing the following: 120 mM KCl, 10 mM HEPES, 10 mM EGTA, 6.19 mM $CaCl_2$,1.44 mM $MgCl_2$, pH 7.4, with KOH. In ***B***, electrodes were filled with an internal solution composed of the following: 140 mM KCl, 10 mM HEPES, 0.05 mM EGTA, 1.5 mM Na_2ATP, 2.34 mM $MgCl_2$, pH 7.4, adjusted with KOH. Cells were bathed in an external solution containing the following: 140 mM KCl, 10 mM HEPES, 10 mM EGTA, 2.5 mM $CaCl_2$, 1.2 mM $MgCl_2$, pH 7.4, with KOH. Apamin (100 nM) reduced both SK2 channel-mediated K^+ currents in the presence of calcium (***A***) and glutamate (L-glut, 1 mM)-mediated activation of SK2 channel in the absence of calcium (***B***). ***C***, Quantification of the current differences observed in ***A*** and ***B***. The current at the potential of −80 mV was quantified and expressed as mean ± SEM ($n = 4$). The asterisks denote data significantly different (*$p <$ 0.05, ***$p < 0.001$, 1-way ANOVA with a Bonferroni's *post hoc* test).

holder, placed on an inverted Axio Observer microscope, and continuously superfused. Electrodes (4–6 MΩ) were fabricated from borosilicate glass (GC120F-10; Harvard Apparatus). Whole-cell voltage-clamp recordings were made using electrodes filled with an internal solution composed of the following: 120 mM KCl, 10 mM HEPES, 10 mM ethylene glycol tetraacetic acid (EGTA), 1.5 mM Na_2ATP, 9.65 mM $CaCl_2$ (estimated free $[Ca^{2+}]_I$, 1 μM), 2.34 mM $MgCl_2$, pH 7.4, adjusted with KOH. Cells were then bathed in a control external solution that consisted of the following: 120 mM KCl, 10 mM HEPES, 10 mM EGTA, 6.19 mM $CaCl_2$ (estimated free $[Ca^{2+}]_i$, 60 nM), 1.44 mM $MgCl_2$, pH 7.4, with KOH. Recordings of whole-cell current were filtered at 2 kHz using an Axopatch 200B amplifier and a Digidata1440A Series interface board and analyzed off-line using pClamp10 software (Molecular Devices). All drugs were applied in the superfusing solution at the indicated concentrations.

For recordings from primary hippocampal neurons, coverslips were mounted in a custom-built recording chamber placed on the stage of an inverted microscope (IX50, Olympus). Cells were continuously superfused with an extracellular solution containing the following: 140 mM NaCl, 3.5 mM KCl, 10 mM HEPES, 1 mM tetraethylammonium, 20 mM D-glucose, 2.5 mM $CaCl_2$, and 1.5 mM $MgCl_2$, pH 7.4, with NaOH (300–305 mOsmol/kg at 20°C). Intracellular electrodes were filled with a solution containing the following: 135 mM K-gluconate, 10 mM KCl, 10 mM HEPES, 1 mM $MgCl_2$, 2 mM Na_2-ATP, 0.4 mM Na_3-GTP, pH 7.2, with KOH (280–290 mOsmol/kg). To suppress the slow Ca^{2+}-dependent K^+ afterhyperpolarization current, 50 μM CPT-cAMP was included in the intracellular solution. Interestingly, 8-(4-chlorophenylthio)-cAMP-mediated activation of PKA does not affect hippocampal SK2 channels that are activated by somatic voltage clamp (J.P. Adelman, unpublished observations). Voltage-clamp experiments were performed on pyramidal cells at 21 DIV and currents were filtered at 1 kHz and recorded at 2 kHz using an Axopatch 200B and a Digidata1440A interface board and pClamp10 software. Neurons were clamped at a membrane holding potential of −50 mV and repetitively depolarized to +30 mV for 200 ms at a frequency of 0.03 Hz to activate voltage-gated Ca^{2+} channels. After each depolarization, the membrane potential was stepped back to −50 mV, where the apamin-sensitive SK current I_{SK} was observed as an outward tail current. Experiments were conducted in the presence of 0.5 μM TTX, 50 μM APV, and 50 μM NBQX to block voltage-gated Na^+ channels, NMDA receptors, and AMPA receptors, respectively. (*R*,*S*)-2-chloro-5-hydroxyphenylglycine (CHPG; 1 mM) was bath applied to activate mGlu$_5$ receptors. At the end of the experiment, apamin (100 nM) was applied to block the SK current. Series resistance (11–20 MΩ) was monitored at regular intervals throughout the recording and presented minimal variations (10–18%) in the analyzed cells. Data are reported without corrections for liquid junction potentials and was analyzed using IGOR Pro (Wavemetrics) together with Neuromatic (Jason Rothman, University College London).

Statistics. The number of samples (n) in each experimental condition is indicated in figure legends. When two experimental conditions were compared, statistical analysis was performed using an unpaired t test. Otherwise, statistical analysis was performed by one-way ANOVA followed by Bonferroni's *post hoc* test. Statistical significance was set as $p < 0.05$.

Results

Coclustering of SK2 channels and mGlu$_5$ receptors in dendritic spines

Light-level immunohistochemistry showed that SK2 channels and mGlu$_5$ receptors are widely distributed throughout the hippocampus, with particularly high expression in the CA1 region (Fig. 1*A*,*B*). Using high-resolution immunoelectron microscopy, we previously reported, separately, the localization of SK2 channels (Lin et al., 2008; Ballesteros-Merino et al., 2012) and mGlu$_5$ receptors (Lujan et al., 1996, 1997) in dendritic spines of hippocampal pyramidal cells. Thus, we showed that SK2 channels reside in both the postsynaptic membrane and in presynaptic sites, while mGlu$_5$ receptors are mainly localized perisynaptically (Lujan et al., 1997; Lin et al., 2008; Ballesteros-Merino et al., 2012). To determine their relative spatial relationship within the spine compartment, we performed immunogold electron microscopy using SDS-FRL (Fujimoto, 1995). Immunoparticles for SK2 channels and mGlu$_5$ receptors were localized at the protoplasmic face (Fig. 1*C*), reflecting the intracellular location of

the epitopes for the two proteins. In addition, immunogold particles for both proteins were concentrated in dendritic spines of pyramidal cells showing either scattered or clustered patterns of distribution (Fig. 1*C–E*). Indeed, the particles for SK2 channels and mGlu$_5$ receptors were coclustered, with the distances between SK2 channels and mGlu$_5$ receptors being shorter than those found for SK2 or mGlu$_5$ receptors alone (Fig. 1*F*). Importantly, the specificity of immunolabeling using the SDS-FRL technique was controlled and confirmed in samples from SK2 channel-null or mGlu$_5$ receptor-null mice (Fig. 1*G*,*H*). These results revealed close, selective anatomical proximity for SK2 channels and mGlu$_5$ receptors in spines, suggesting that they may coassemble. This was tested by coimmunoprecipitation from hippocampal protein extracts. When the anti-mGlu$_5$ receptor antibody was used for immunoprecipitation, a protein of ~130 kDa corresponding to the mGlu$_5$ receptor (Fig. 2*A*, IP: 2, IB: anti-mGluR$_5$) was detected in the precipitate. Further, probing the precipitate with anti-SK2 antibody revealed a band of ~65 kDa, consistent with the predicted size of the SK2 channel. Coimmunoprecipitation of the two proteins was confirmed by reversing the order; using the anti-SK2 channel antibody it was coimmunoprecipitated the mGlu$_5$ receptor (Fig. 2*A*, IP: 3, IB: anti-mGluR$_5$). Control experiments used IgG for immunoprecipitation and validated specificity (Fig. 2*A*, IP: 1, IB: anti-mGluR$_5$). These results demonstrate that SK2 channels and mGlu$_5$ receptors closely colocalize in spines and coassemble into stable protein–protein complexes in the hippocampus.

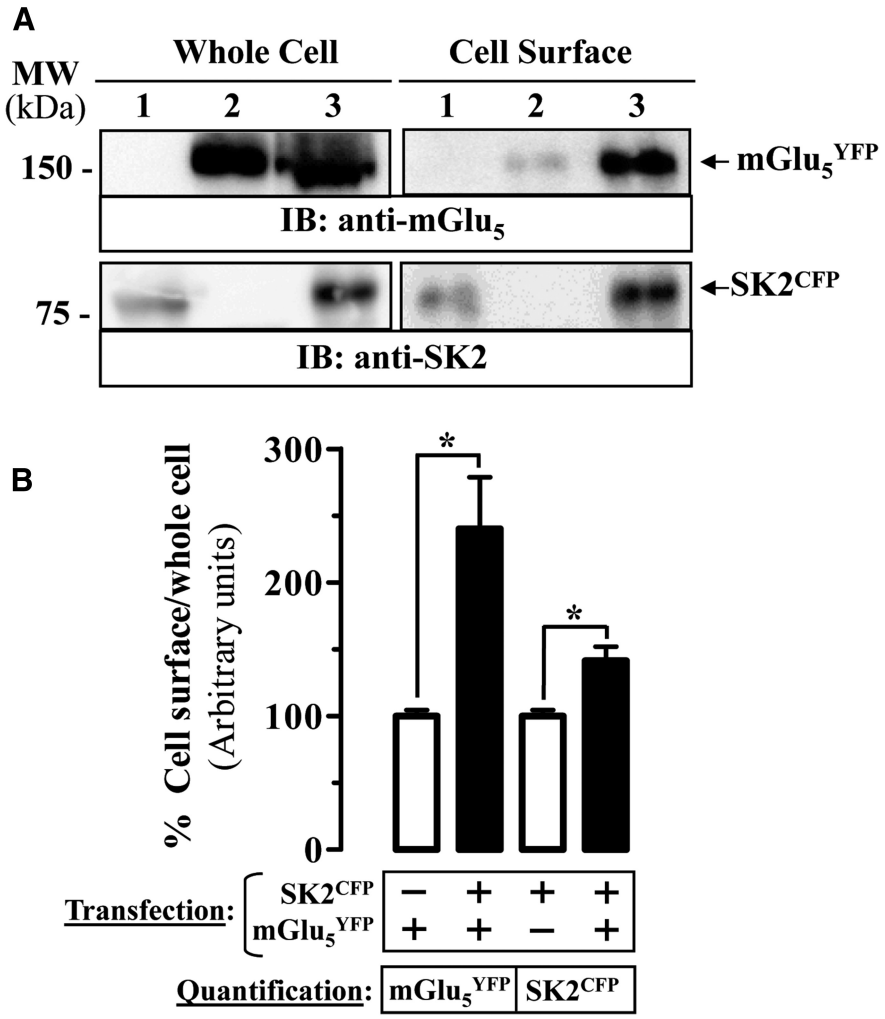

Figure 5. SK2 channels potentiate mGlu$_5$ receptor cell-surface targeting. ***A***, HEK-293T cells were transiently transfected with SK2^{CFP} channels (lane 1), mGlu$_5^{YFP}$ receptors (lane 2), or SK2^{CFP} plus mGlu$_5^{YFP}$ receptors (lane 3). Cell-surface protein labeling was performed as described in Materials and Methods. Crude extracts and biotinylated proteins were subsequently analyzed by SDS-PAGE and immunoblotted using a rabbit anti-mGlu$_5$ receptor antibody or rabbit anti-SK2 channel antibody. The primary bound antibody was detected using an HRP-conjugated goat anti-rabbit antibody (1:30,000). The immunoreactive bands were visualized by chemiluminescence. ***B***, Quantification of mGlu$_5$ receptor and SK2 channel cell-surface expression. The intensities of the immunoreactive bands on immunoblotted membranes corresponding to crude extracts and biotinylated protein were measured by densitometric scanning. Cell-surface receptor and channel values were normalized using the amount of mGlu$_5$ receptors or SK2 channels in the crude extract for each sample. The data indicate the mean ± SEM of six independent experiments. The asterisk indicates statistically significant differences from the respective control condition ($p < 0.05$; Student's *t* test).

SK2 channels and mGlu$_5$ receptors coassemble in HEK-293T cells

Next, we investigated whether coexpression of SK2 channels and mGlu$_5$ receptors was sufficient for coassembly. Thus, SK2^{CFP} channel and mGlu$_5^{YFP}$ receptor constructs were coexpressed in HEK-293T cells, and subcellular distribution was examined using confocal microscopy. This revealed a marked overlap in the distribution of the two proteins at both the plasma membrane and in intracellular organelles (Fig. 2*B*). Subsequent coimmunoprecipitation experiments from cells expressing doubly tagged SK2 channels (SK2$^{YFP/CFP}$ channel) and untagged mGlu$_5$ receptors showed that the anti-SK2 channel antibody coimmunoprecipitated the mGlu$_5$ receptors (Fig. 2*C*, IP: anti-SK2, lane 3, IB: anti-mGlu$_5$), and that the anti-mGlu$_5$ receptor antibody also coimmunoprecipitated the SK2$^{YFP/CFP}$ channels (Fig. 2*C*, IP: anti-mGlu$_5$, lane 3, IB: anti-SK2).

Although the use of biochemical approaches to demonstrate protein–protein interactions has been widely used, it might have some disadvantages as the cellular structure is destroyed by detergent treatment. Thus, to assess whether SK2 channels and mGlu$_5$ receptors oligomerize in living cells, biophysical approaches were performed. Therefore, the formation of the SK2/mGlu$_5$ channel–receptor oligomer was first assessed by means of FRET experiments. To this end, HEK-293T cells were transiently transfected with SK2^{CFP} channel and mGlu$_5^{YFP}$ receptor constructs, and coassembly was evidenced by the FRET engaged between the fluorescent proteins, measured by recovery of the CFP emission after photobleaching of YFP (Fig. 3*A*). In contrast, the photobleaching protocol applied to cells expressing only SK2^{CFP} channels did not change the emission intensity of CFP (data not shown). Also, when the SK2^{CFP} channel was coexpressed with an unrelated transmembrane protein, CD4^{YFP}, the FRET efficiency was significantly lower than that obtained when coexpressing SK2^{CFP} and mGluR$_5^{YFP}$ constructs (Fig. 3*B*). Subsequently, we demonstrated this close proximity of SK2 channels and mGlu$_5$ receptors (i.e., <10 nm) by means of a BRET approach. Accordingly, in cells cotransfected with a constant amount of the mGlu5

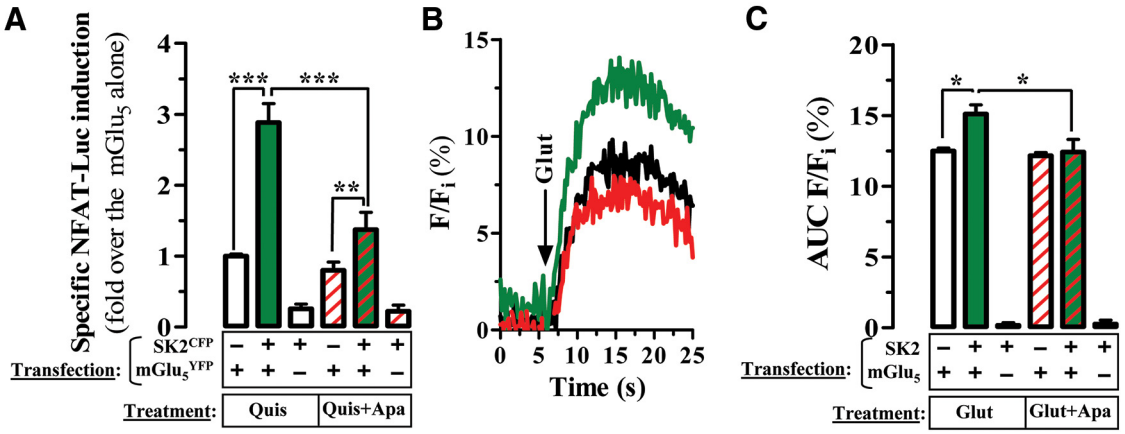

Figure 6. SK2 channels potentiate mGlu$_5$ receptor functioning. ***A***, Determination of mGlu$_5$ receptor-mediated intracellular calcium accumulation by means of a luciferase reporter assay system. HEK-293T cells were transiently transfected with the firefly luciferase-encoding plasmid (pGL4-NFAT-luc2p) with mGlu$_5^{YFP}$ receptors, with SK2^{CFP} channels, or with mGlu$_5^{YFP}$ receptors plus SK2^{CFP} channels. Thirty-six hours after transfection, cells were treated 6 h with the mGlu$_5$ receptor agonist L-quisqualic acid (100 μM) in presence or absence of apamin (100 nM). Light emission is presented as the fold increase over basal levels of the effect of mGlu$_5$ receptors alone. The data are expressed as the mean ± SEM of three independent experiments. The asterisks indicate statistically significant differences (**$p < 0.01$, ***$p < 0.001$, 1-way ANOVA with a Bonferroni's *post hoc* test). ***B***, Representative mGlu$_5$ receptor-mediated intracellular Ca^{2+} accumulation determined by Fluo4 assays. HEK-293T cells were transiently transfected with mGlu$_5$ receptors (black trace) or mGlu$_5$ receptors plus SK2 channels (green and red traces). Cells were loaded with Fluo4-NW dye and challenged with L-glutamate (Glut, 1 mM) in the absence (black and green traces) or presence of apamin (100 nM, red trace). The $[Ca^{2+}]_i$ dynamics is shown as changes in fluorescence of the Fluo4 signal (F) expressed as percentage of the maximal Ca^{2+} influx elicited by ionomycin (F_i) in each experimental condition. ***C***, Quantification of the mGlu$_5$ receptor-mediated $[Ca^{2+}]$i accumulation measured by Fluo4. The integrated area under the curve (AUC) of the normalized mGlu$_5$ receptor-mediated Fluo4 signal (F) is expressed as percentage of the corresponding ionomycin signal (F_i) for each transfection and treatment. The data are expressed as the mean ± SEM of four independent experiments. The asterisk indicates statistically significant differences (*$p < 0.05$, 1-way ANOVA with a Bonferroni's *post hoc* test).

receptor fused to luciferase (mGlu$_5^{Rluc}$ receptor) and increasing amounts of the SK2$^{YFP/CFP}$ channel there was a positive and saturable BRET signal (Fig. 3*C*); while in cells cotransfected with the mGlu$_5^{Rluc}$ receptor and increasing amounts of a noninteracting protein (GABA$_2$R^{YFP}) the BRET signal was quasilinear (Fig. 3*C*). Together, these results demonstrate that coexpression of SK2 channels and mGlu$_5$ receptors is sufficient for the coassembly of the two proteins.

Functional coupling between SK2 channels and mGlu$_5$ receptors

The formation of SK2 channel–mGlu$_5$ receptor molecular complexes in hippocampus and in transfected cells suggested that there might exist a functional coupling between them, as mGlu$_5$ receptor activation promotes Ca^{2+} release from internal stores. Therefore, we performed whole-cell voltage-clamp recordings from transiently transfected HEK-293T cells. In cells expressing the SK2 channel alone, recordings with 2.5 mM free Ca^{2+} in the internal pipette solution display inwardly rectifying currents to voltage ramps between −80 and +80 mV that were largely suppressed by apamin application (100 nM; Fig. 4*A*). In contrast, whole-cell voltage ramps applied to cells coexpressing SK2 channels and mGlu$_5$ receptors in a Ca^{2+}-free internal solution (50 μM EGTA) yielded lineal unspecific small-leak currents that were not affected by apamin (Fig. 4*B*, black trace). However, after application of L-glutamate (1 mM), voltage ramps evoked large apamin-sensitive currents (Fig. 4*B*,*C*). In addition, to investigate the source of the Ca^{2+} that activated the SK2 current, under these same experimental conditions with EGTA in the recording pipette, we performed experiments in which cells were pretreated for 30–60 min with thapsigargin (2 μM), a noncompetitive sarcoendoplastic reticulum Ca^{2+}-ATPase inhibitor, which discharges intracellular Ca^{2+} stores. A significant reduction in the number of mGlu$_5$ receptor-expressing cells showing glutamate-mediated SK2 activation was observed (from 38% in control cells to 9% in thapsigargin-treated ones; $p < 0.05$; one-tailed Fisher's exact test). These results show that activation of mGlu$_5$ receptors triggers coexpressed SK2 channel currents in the absence of Ca^{2+} influx and via the release of Ca^{2+} from intracellular stores.

Coexpression enhances plasma membrane expression

Interestingly, the whole-cell SK2 channel current amplitudes were larger for cells coexpressing mGlu$_5$ receptors (see above), suggesting that coexpression with the mGlu$_5$ receptor may promote SK2 channel surface expression. To determine whether coexpression affected the levels of SK2 channels or mGlu$_5$ receptors in the plasma membrane, cell-surface proteins were isolated following biotinylation and the amounts of SK2 channels or mGlu$_5$ receptors, as a fraction of the total in the cell lysate, were determined by Western blotting. The results showed that coexpression reciprocally enhanced the amount of SK2 channels or mGlu$_5$ receptors inserted into the membrane (~1.5-fold and ~2.5-fold over the basal, respectively; Fig. 5*A*,*B*). To test whether the enhanced surface expression was accompanied by increased mGlu$_5$ receptor signaling, we determined mGlu$_5$ receptor-mediated calcium responses by two different and complementary approaches. Initially, we used a homogenous bioluminescent reporter assay system using a NFAT response element controlling luciferase gene expression. To this end, cells were additionally transfected with an NFAT-luciferase reporter plasmid (pGL4-NFAT-RE/luc2p). In these cells, activation of the mGlu$_5$ receptor via application of the agonist quisqualic acid (100 μM) increased intracellular Ca^{2+}, which enhanced NFAT-sensitive expression of luciferase (Fig. 6*A*). Consistent with the larger SK2 channel currents and the increased amounts of plasma membrane expression of both SK2 channels and mGlu$_5$ receptors, coexpression increased mGlu$_5$ receptor signaling (~3-fold over the basal; Fig. 6*A*). Surprisingly, in cells coexpressing mGlu$_5$ receptors and SK2 channels, apamin application significantly reduced mGlu$_5$ receptor signaling (Fig. 5*C*). Subsequently, we assessed the impact of SK2 channel expression in mGlu$_5$ receptor-mediated intracellular calcium mobilization by means of mGlu$_5$ receptor

Fluo4 determinations. Thus, in Fluo4-loaded cells, the activation of the mGlu$_5$ receptor increased intracellular Ca^{2+} (Fig. 6*B*, black trace), as expected. Consistent with the results obtained in the NFAT experiments, coexpression significantly increased mGlu$_5$ receptor-mediated intracellular calcium accumulation (Fig. 6*B*,*C*). Again, in coexpressing cells, the apamin treatment significantly reduced mGlu$_5$ receptor signaling (Fig. 6*B*,*C*).

SK2 channel–mGlu$_5$ receptor coupling in hippocampal neurons

The results obtained in a heterologous system confirmed that SK2 channels and mGlu$_5$ receptors coassemble into functionally interacting complexes at the plasma membrane level. To determine whether this also occurs in cultured hippocampal neurons, we first examined the subcellular distribution of these two proteins by immunocytochemistry. This revealed an overlap in the distribution of mGlu$_5$ receptors and SK2 channels in the cell body and throughout distal neurites (Fig. 7*A*). Subsequently, we investigated mGlu$_5$ receptor modulation of SK2 channel function by measuring the effect of the mGlu$_5$ receptor agonist CHPG on the SK channel current amplitude. CHPG (1 mM) application induced an increase of the SK channel current (Fig. 7*B*,*C*), which was completely blocked by apamin (100 nM; Fig. 7*B*).

Additionally, by monitoring mGlu$_5$ receptor-mediated inositol phosphate accumulation, we investigated whether SK2 channel gating impacts mGlu$_5$ receptor function. IP_1 accumulation was measured, instead of IP_3, to monitor the activity of G-protein-coupled receptors linked to phospholipase C in cells treated with LiCl to inhibit inositol monophosphatase (Trinquet et al., 2006). Incubation of cultured hippocampal neurons with CHPG enhanced IP_1 accumulation over basal levels (1.8 ± 0.2%, $n = 8$, $p < 0.01$; Fig. 7*D*). Importantly, apamin treatment of the hippocampal neurons prevented the CHPG-mediated IP_1 accumulation, thus suggesting that the endogenous mGlu$_5$ receptor requires SK2 channel activity.

Discussion

The results presented here show that SK2 channels and mGlu$_5$ receptors coassemble and bidirectionally regulate its activity. Hence, activation of mGlu$_5$ receptors mobilizes intracellular Ca^{2+}, which gates the SK2 channel, while blocking SK2 channels with apamin limits mGlu$_5$ receptor signaling.

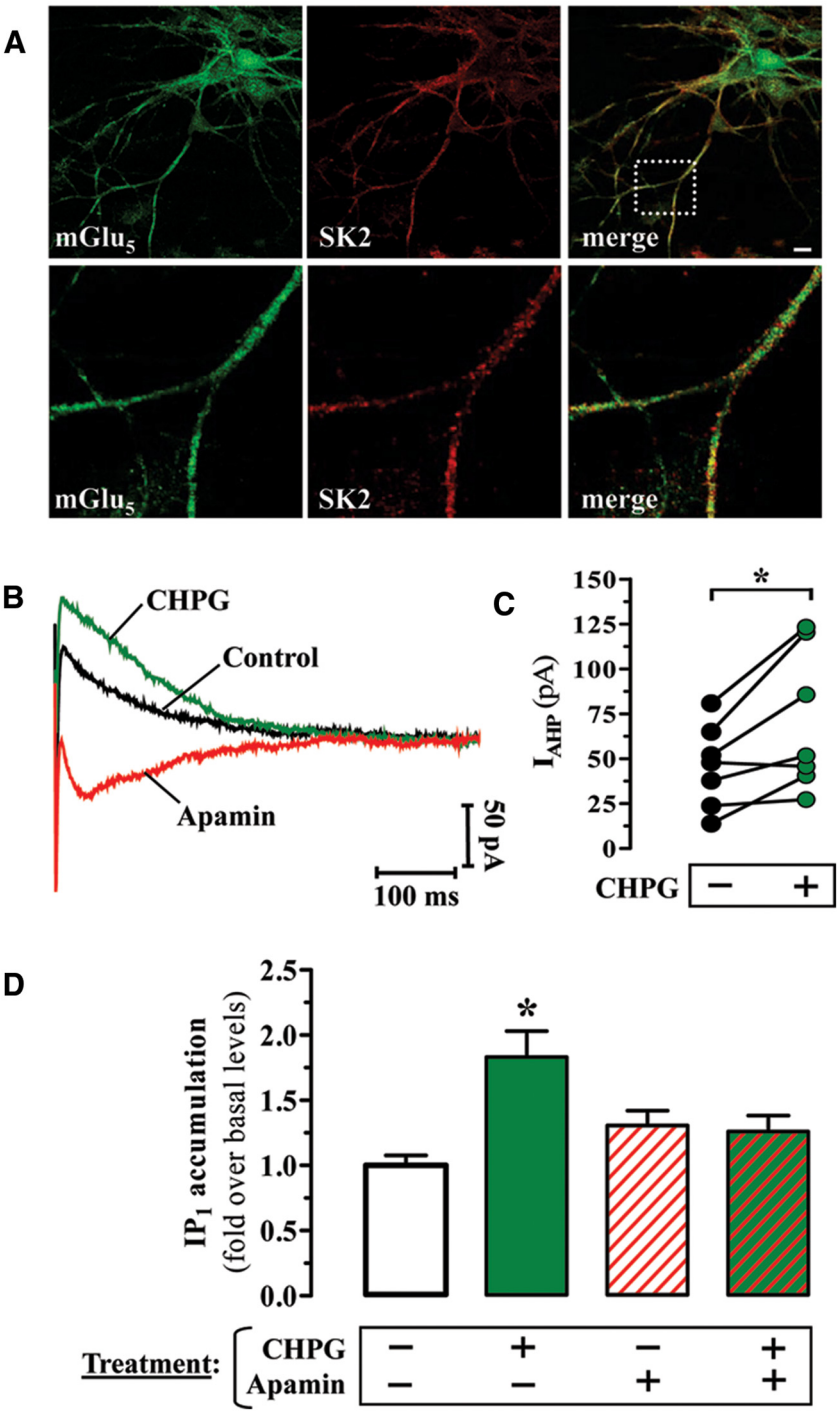

Figure 7. SK2 channels and mGlu$_5$ receptors functionally interact in hippocampal neurons. ***A***, Codistribution of SK2 channels and mGlu$_5$ receptors in cultured hippocampal neurons. Primary hippocampal neurons were fixed, permeabilized, and immunostained using guinea pig anti-SK2 channel (1 μg/ml) and rabbit anti-mGlu$_5$ receptor (1 μg/ml) antibodies. Primary antibodies were detected using Cy2-conjugated donkey anti-rabbit antibody (1:200) and Cy3-conjugated donkey anti-guinea pig antibody (1:200). Neurons were analyzed by double immunofluorescence with a confocal microscopy. Images show mGlu$_5$ receptors in green and SK2 channels in red. Superimposition of images (merge) reveals codistribution in yellow. A magnification of a region of interest (white dashed square) is shown in lower panels. Scale bar, 10 μm. ***B***, Effect of mGlu$_5$ receptor activation on the afterhyperpolarization current (I_{AHP}) amplitude in cultured hippocampal neurons. Typical experiment showing the I_{AHP} (black line; average of 4 traces) increment after bath application of 1 mM CHPG (green line; average of 5 traces). The I_{AHP} was completely blocked after the addition of 100 nM apamin (red line; average of 4 traces). ***C***, Quantification of the CHPG-mediated increment on the I_{AHP}. The asterisk indicates statistically significant difference from the control condition ($p < 0.05$; paired Student's *t* test). ***D***, Effect of apamin on CHPG-mediated IP_1 accumulation in hippocampal neurons. Neurons were incubated with CHPG (333 μM) in presence or absence of apamin (100 nM) and the accumulation of IP_1 was determined as described in the Materials and Methods section. The results are presented as the fold increase over basal levels of IP_1 in vehicle-treated neurons. The asterisk indicates statistically significant difference from all other three experimental conditions (*$p < 0.05$, 1-way ANOVA with a Bonferroni's *post hoc* test).

In hippocampus, double-label immunogold electron microscopy using SDS-FRL revealed close coclustering of SK2 channels and mGlu$_5$ receptors in dendritic spines of CA1 pyramidal neurons. Together with previously published findings, it is likely that the two proteins are in very close anatomical proximity near, but not in, the PSD. The ability to coimmunoprecipitate SK2 channels and mGlu$_5$ receptors from hippocampus and following coexpression in HEK-293T cells supports their physical association and suggests that coexpression of only SK2 channels and mGlu$_5$ receptors is sufficient for coassembly. Notably, coexpression of SK2 channels and mGlu$_5$ receptors also promoted plasma membrane expression of both proteins, thus substantiating the observed channel–receptor interaction.

SK2 channel and mGlu$_5$ receptor coassembly results in functional coupling. Thus, in transfected cells and primary hippocampal neurons, mGlu$_5$ receptor stimulation mobilized intracellular Ca^{2+} and robustly activated SK2 channels, consistent with previous reports in prefrontal cortex and hippocampus (Hagenston et al., 2008; El-Hassar et al., 2011). Remarkably, mGlu$_5$ receptor function was modulated by SK2 channel activity. Thus, blocking the SK2 channels with apamin regulated mGlu$_5$ receptor-mediated signal transduction both in transfected cells and in primary hippocampal neurons. While the molecular basis is currently being studied, these results demonstrate that the physical coassembly of SK2 channels and mGlu$_5$ receptors enables bidirectional regulation.

In many central neurons, apamin-sensitive SK channels contribute to the afterhyperpolarization that follows a single action potential or a burst of action potentials (for review, see Adelman et al., 2012). However, this is not the case in CA1 pyramidal neurons (Gu et al., 2005, 2008; J. P. Adelman, unpublished observations), where SK2-containing channels contribute to synaptic and dendritic functions. Thus, in spines they modulate synaptic responses and the induction and expression of plasticity (Stackman et al., 2002; Ngo-Anh et al., 2005; Lin et al., 2008), while in dendrites they modulate the time course of branch-specific Ca^{2+} plateau potentials (Cai et al., 2004). Interestingly, the apamin-sensitive SK channel activity recorded in whole-cell current clamp that requires Ca^{2+} influx through NMDA receptors, and the apamin-sensitive currents recorded in voltage clamp that are hampered by blocking voltage-gated Ca^{2+} channels reflect distinct populations of SK channels. Indeed, selectively eliminating synaptic SK channels does not affect the apamin-sensitive currents recorded at the soma (Allen et al., 2011). The present findings in cultured hippocampal neurons shows a mGlu$_5$ receptor-dependent increase of the SK current activated in voltage clamp, suggesting a third population of apamin-sensitive SK channels that are coupled to mGlu$_5$ receptor-dependent IP_3-mediated Ca^{2+} mobilization. The most parsimonious consequence of mGlu$_5$ receptor-dependent activation of SK channels would be to hyperpolarize the neuron and decrease excitability. Yet, in hippocampal slices there may be a biphasic response, first hyperpolarizing and then depolarizing, reflecting the sequential activity of SK and transient receptor potential canonical channels (El-Hassar et al., 2011). Moreover, while mGlu$_5$ receptor activation may mediate increased SK channel activity to decrease excitability, mGlu$_5$ receptor activity may also suppress the afterhyperpolarization current, increasing excitability (Mannaioni et al., 2001). Accordingly, in layer V pyramidal neurons, activation of mGlu$_5$ receptors may induce a long-term potentiation of intrinsic excitability that reflects downregulation of SK channels (Sourdet et al., 2003). In hippocampus, both SK channels and mGlu$_5$ receptors influence learning and memory (Stackman et al., 2002; Naie and Manahan-Vaughan, 2004; Hayashi et al., 2007; Gil-Sanz et al., 2008; Allen et al., 2011), suggesting that the mGlu$_5$ receptor coupling to SK2 channel activity may play an important role in encoding hippocampal information.

References

Adelman JP, Maylie J, Sah P (2012) Small-conductance Ca^{2+}-activated K+ channels: form and function. Annu Rev Physiol 74:245–269. CrossRef Medline

Allen D, Bond CT, Luján R, Ballesteros-Merino C, Lin MT, Wang K, Klett N, Watanabe M, Shigemoto R, Stackman RW Jr, Maylie J, Adelman JP (2011) The SK2-long isoform directs synaptic localization and function of SK2-containing channels. Nat Neurosci 14:744–749. CrossRef Medline

Ballesteros-Merino C, Lin M, Wu WW, Ferrandiz-Huertas C, Cabañero MJ, Watanabe M, Fukazawa Y, Shigemoto R, Maylie J, Adelman JP, Luján R (2012) Developmental profile of SK2 channel expression and function in CA1 neurons. Hippocampus 22:1467–1480. CrossRef Medline

Borroto-Escuela DO, Romero-Fernandez W, Tarakanov AO, Ciruela F, Agnati LF, Fuxe K (2011) On the existence of a possible A2A-D2-beta-Arrestin2 complex: A2A agonist modulation of D2 agonist-induced beta-arrestin2 recruitment. J Mol Biol 406:687–699. CrossRef Medline

Cabello N, Gandía J, Bertarelli DC, Watanabe M, Lluís C, Franco R, Ferré S, Luján R, Ciruela F (2009) Metabotropic glutamate type 5, dopamine D(2) and adenosine A(2a) receptors form higher-order oligomers in living cells. J Neurochem 109:1497–1507. CrossRef Medline

Cai X, Liang CW, Muralidharan S, Muralidharan S, Kao JP, Tang CM, Thompson SM (2004) Unique roles of SK and Kv4.2 potassium channels in dendritic integration. Neuron 44:351–364. CrossRef Medline

Canals M, Marcellino D, Fanelli F, Ciruela F, de Benedetti P, Goldberg SR, Neve K, Fuxe K, Agnati LF, Woods AS, Ferré S, Lluis C, Bouvier M, Franco R (2003) Adenosine A2A-dopamine D2 receptor-receptor heteromerization: qualitative and quantitative assessment by fluorescence and bioluminescence energy transfer. J Biol Chem 278:46741–46749. CrossRef Medline

Ciruela F, Soloviev MM, Chan WY, McIlhinney RA (2000) Homer-1c/Vesl-1L modulates the cell surface targeting of metabotropic glutamate receptor type 1alpha: evidence for an anchoring function. Mol Cell Neurosci 15:36–50. CrossRef Medline

Ciruela F, Burgueño J, Casadó V, Canals M, Marcellino D, Goldberg SR, Bader M, Fuxe K, Agnati LF, Lluis C, Franco R, Ferré S, Woods AS (2004) Combining mass spectrometry and pull-down techniques for the study of receptor heteromerization. Direct epitope-epitope electrostatic interactions between adenosine A2A and dopamine D2 receptors. Anal Chem 76:5354–5363. CrossRef Medline

El-Hassar L, Hagenston AM, D'Angelo LB, Yeckel MF (2011) Metabotropic glutamate receptors regulate hippocampal CA1 pyramidal neuron excitability via Ca(2)(+) wave-dependent activation of SK and TRPC channels. J Physiol 589:3211–3229. CrossRef Medline

Faber ES, Delaney AJ, Sah P (2005) SK channels regulate excitatory synaptic transmission and plasticity in the lateral amygdala. Nat Neurosci 8:635–641. CrossRef Medline

Fujimoto K (1995) Freeze-fracture replica electron microscopy combined with SDS digestion for cytochemical labeling of integral membrane proteins. Application to the immunogold labeling of intercellular junctional complexes. J Cell Sci 108:3443–3449. Medline

Gandia J, Galino J, Amaral OB, Soriano A, Lluís C, Franco R, Ciruela F (2008) Detection of higher-order G protein-coupled receptor oligomers by a combined BRET-BiFC technique. FEBS Lett 582:2979–2984. CrossRef Medline

Gil-Sanz C, Delgado-García JM, Fairén A, Gruart A (2008) Involvement of the mGluR1 receptor in hippocampal synaptic plasticity and associative learning in behaving mice. Cereb Cortex 18:1653–1663. CrossRef Medline

Giménez-Llort L, Schiffmann SN, Shmidt T, Canela L, Camón L, Wassholm M, Canals M, Terasmaa A, Fernández-Teruel A, Tobeña A, Popova E, Ferré S, Agnati L, Ciruela F, Martínez E, Scheel-Kruger J, Lluis C, Franco R, Fuxe K, Bader M (2007) Working memory deficits in transgenic rats overexpressing human adenosine A2A receptors in the brain. Neurobiol Learn Mem 87:42–56. CrossRef Medline

Gu N, Vervaeke K, Hu H, Storm JF (2005) Kv7/KCNQ/M and HCN/h, but not KCa2/SK channels, contribute to the somatic medium after-

hyperpolarization and excitability control in CA1 hippocampal pyramidal cells. J Physiol 566:689–715. CrossRef Medline

Gu N, Hu H, Vervaeke K, Storm JF (2008) SK (KCa2) channels do not control somatic excitability in CA1 pyramidal neurons but can be activated by dendritic excitatory synapses and regulate their impact. J Neurophysiol 100:2589–2604. CrossRef Medline

Hagenston AM, Fitzpatrick JS, Yeckel MF (2008) MGluR-mediated calcium waves that invade the soma regulate firing in layer V medial prefrontal cortical pyramidal neurons. Cereb Cortex 18:407–423. CrossRef Medline

Hayashi K, Yoshihara T, Ichitani Y (2007) Involvement of hippocampal metabotropic glutamate receptors in radial maze performance. Neuroreport 18:719–723. CrossRef Medline

Hollmann M, Heinemann S (1994) Cloned glutamate receptors. Annu Rev Neurosci 17:31–108. CrossRef Medline

Köhler M, Hirschberg B, Bond CT, Kinzie JM, Marrion NV, Maylie J, Adelman JP (1996) Small-conductance, calcium-activated potassium channels from mammalian brain. Science 273:1709–1714. CrossRef Medline

Lin MT, Luján R, Watanabe M, Adelman JP, Maylie J (2008) SK2 channel plasticity contributes to LTP at Schaffer collateral-CA1 synapses. Nat Neurosci 11:170–177. CrossRef Medline

López-Hernández T, Sirisi S, Capdevila-Nortes X, Montolio M, Fernández-Dueñas V, Scheper GC, van der Knaap MS, Casquero P, Ciruela F, Ferrer I, Nunes V, Estévez R (2011) Molecular mechanisms of MLC1 and GLIALCAM mutations in megalencephalic leukoencephalopathy with subcortical cysts. Hum Mol Genet 20:3266–3277. CrossRef Medline

Luján R, Ciruela F (2001) Immunocytochemical localization of metabotropic glutamate receptor type 1 alpha and tubulin in rat brain. Neuroreport 12:1285–1291. CrossRef Medline

Lujan R, Nusser Z, Roberts JD, Shigemoto R, Somogyi P (1996) Perisynaptic location of metabotropic glutamate receptors mGluR1 and mGluR5 on dendrites and dendritic spines in the rat hippocampus. Eur J Neurosci 8:1488–1500. CrossRef Medline

Luján R, Roberts JD, Shigemoto R, Ohishi H, Somogyi P (1997) Differential plasma membrane distribution of metabotropic glutamate receptors mGluR1 alpha, mGluR2 and mGluR5, relative to neurotransmitter release sites. J Chem Neuroanat 13:219–241. CrossRef Medline

Mannaioni G, Marino MJ, Valenti O, Traynelis SF, Conn PJ (2001) Metabotropic glutamate receptors 1 and 5 differentially regulate CA1 pyramidal cell function. J Neurosci 21:5925–5934. Medline

Martín R, Durroux T, Ciruela F, Torres M, Pin JP, Sánchez-Prieto J (2010) The metabotropic glutamate receptor mGlu7 activates phospholipase C, translocates munc-13-1 protein, and potentiates glutamate release at cerebrocortical nerve terminals. J Biol Chem 285:17907–17917. CrossRef Medline

Mayer ML, Westbrook GL (1987) The physiology of excitatory amino acids in the vertebrate central nervous system. Prog Neurobiol 28:197–276. CrossRef Medline

Naie K, Manahan-Vaughan D (2004) Regulation by metabotropic glutamate receptor 5 of LTP in the dentate gyrus of freely moving rats: relevance for learning and memory formation. Cereb Cortex 14:189–198. CrossRef Medline

Nassirpour R, Bahima L, Lalive AL, Lüscher C, Luján R, Slesinger PA (2010) Morphine- and CaMKII-dependent enhancement of GIRK channel signaling in hippocampal neurons. J Neurosci 30:13419–13430. CrossRef Medline

Ngo-Anh TJ, Bloodgood BL, Lin M, Sabatini BL, Maylie J, Adelman JP (2005) SK channels and NMDA receptors form a Ca2+-mediated feedback loop in dendritic spines. Nat Neurosci 8:642–649. CrossRef Medline

Pin JP, Duvoisin R (1995) The metabotropic glutamate receptors: structure and functions. Neuropharmacology 34:1–26. CrossRef Medline

Sourdet V, Russier M, Daoudal G, Ankri N, Debanne D (2003) Long-term enhancement of neuronal excitability and temporal fidelity mediated by metabotropic glutamate receptor subtype 5. J Neurosci 23:10238–10248. Medline

Stackman RW, Hammond RS, Linardatos E, Gerlach A, Maylie J, Adelman JP, Tzounopoulos T (2002) Small conductance Ca^{2+}-activated K+ channels modulate synaptic plasticity and memory encoding. J Neurosci 22:10163–10171. Medline

Stocker M (2004) Ca(2+)-activated K+ channels: molecular determinants and function of the SK family. Nat Rev Neurosci 5:758–770. CrossRef Medline

Tarusawa E, Matsui K, Budisantoso T, Molnár E, Watanabe M, Matsui M, Fukazawa Y, Shigemoto R (2009) Input-specific intrasynaptic arrangements of ionotropic glutamate receptors and their impact on postsynaptic responses. J Neurosci 29:12896–12908. CrossRef Medline

Trinquet E, Fink M, Bazin H, Grillet F, Maurin F, Bourrier E, Ansanay H, Leroy C, Michaud A, Durroux T, Maurel D, Malhaire F, Goudet C, Pin JP, Naval M, Hernout O, Chrétien F, Chapleur Y, Mathis G (2006) D-myo-inositol 1-phosphate as a surrogate of D-myo-inositol 1,4,5-tris phosphate to monitor G protein-coupled receptor activation. Anal Biochem 358:126–135. CrossRef Medline

Uchigashima M, Narushima M, Fukaya M, Katona I, Kano M, Watanabe M (2007) Subcellular arrangement of molecules for 2-arachidonoylglycerol-mediated retrograde signaling and its physiological contribution to synaptic modulation in the striatum. J Neurosci 27:3663–3676. CrossRef Medline

Xia XM, Fakler B, Rivard A, Wayman G, Johnson-Pais T, Keen JE, Ishii T, Hirschberg B, Bond CT, Lutsenko S, Maylie J, Adelman JP (1998) Mechanism of calcium gating in small-conductance calcium-activated potassium channels. Nature 395:503–507. CrossRef Medline